Supporting Information for

Tellurene short-wave infrared photodetector with fast response and High specific detectivity

Yafei Yan[a‡], Kai Xia[b,c‡], Wei Gan[a], Kemeng Yang[a], Gang Li[a], Xi Tang[a], Liang Li[a,c], Changjin Zhang[a,d], Guang Tao Fei[c], Hui Li[a*]*

[a]Institute of Physical Science and Information Technology and Information Materials and Intelligent Sensing Laboratory of Anhui Province, Anhui University, Hefei 230601, China

[b]University of Science and Technology of China, Hefei 230026, P. R. China

[c]Key Laboratory of Materials Physics and Anhui Key Laboratory of Nanomaterials and Nanotechnology, Institute of Solid State Physics, Hefei Institutes of Physical Science, Chinese Academy of Sciences, Hefei 230031, P. R. China

[d]High Magnetic Field Laboratory of Anhui Province, Chinese Academy of Sciences, Hefei 230031, China

‡ These authors contributed equally.

*Correspondence and requests for materials should be addressed to G. F. (email: gtfei@issp.ac.cn) and H. L. (email: huili@ahu.edu.cn).

Experimental section

1. Synthesis and Characterization of 2D Te Nanoflakes

0.1 g of Na_2TeO_3 and 0.072 g of polyvinylpyrrolidone (PVP) (molecular weight 40000) were completely dissolved in 30 mL of deionized water. The aqueous solution was transferred into a Teflon-lined stainless-steel autoclave, followed by adding 3 mL ammonia solution (25% by wt/wt%) and 200 μL - 1 mL hydrazine hydrate (80% by wt/wt%). Then the autoclave is sealed and kept at 180 ^oC for 20 - 48 hours before cooling to room temperature naturally. The obtained solid silver-gray product was centrifuged and precipitated at 5000 rpm/min for 5 minutes and washed three times using deionized water.

Characterization of Te nanoflakes: Te flakes were characterized using optical microscope (Olympus BX53M) for morphology observations, and AFM (Park NX10) for thickness determination. Stoichiometry analyses of as-grown Te nanoflakes were determined by energy dispersive X-ray spectroscopy (EDS) analysis through a field-emission scanning electron microscope (JEOL-7100F). The HRTEM images, SAED and EDX were characterized by TEM (JEM-F200).

2. Angle Resolved Raman Spectra Measurement

Angle resolved Raman spectra were measured at room temperature using Raman system (FST2 Ahdx DZ, Zolix) equipped with a monochromator, with laser wavelength of 532 nm and 100x microscope objective lens. Linear polarizer is placed under the spectrometer to polarize the reflected light in the same direction as the incident light. Angle-resolved Raman peak intensity was measured by rotating the Te nanoflake. The peak intensities of different Raman modes were extracted by using Lorentz fitting and plotted in polar plots.

3. Device Fabrication and Characterization of Te-based Photodetectors

The as-synthesized Te nanoflakes were firstly dispersed into deionized water and dropped onto the SiO_2/Si substrates. Standard electron beam lithography (EBL) and thermal evaporation were adopted for the Cr/Au (10/100 nm) electrodes.

The current - voltage (*I-V*) characteristics and photocurrent response of Te

photodetectors were measured by Keithley semiconductor parameter analyzer (4200-SCS, Keithley Instruments Inc., Cleveland, OH, USA). The chopper is used to control the switch of the light path to produce low-frequency pulse light (GCI-73, Daheng Science & Technology Inc., Beijing, China). The LED light (MDL-III-1550-300mW, CNI., Changchun, China) with a central wavelength of 1550 nm was used as the light source for infrared light illumination.

Supporting Note 1. Schematic illustration of hydrothermal synthesis process

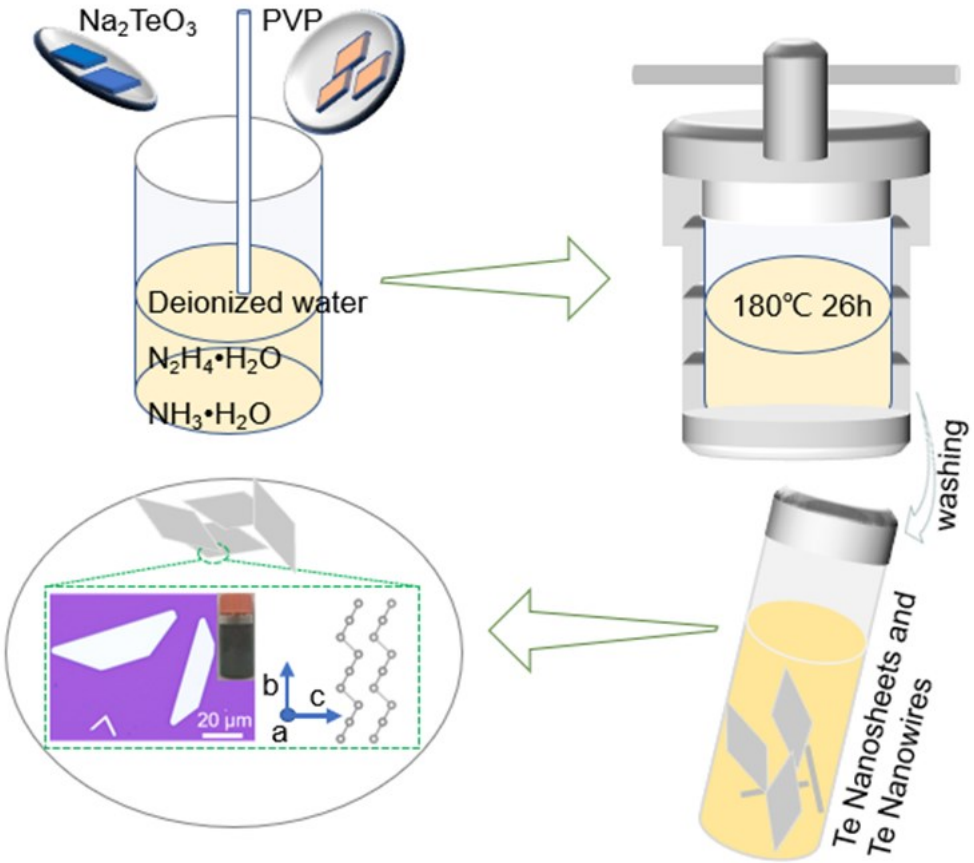

Fig. S1 Schematic illustration for the hydrothermal synthesis of 2D Te nanoflakes.

Supporting Note 2. Schematic illustration of Raman vibrations

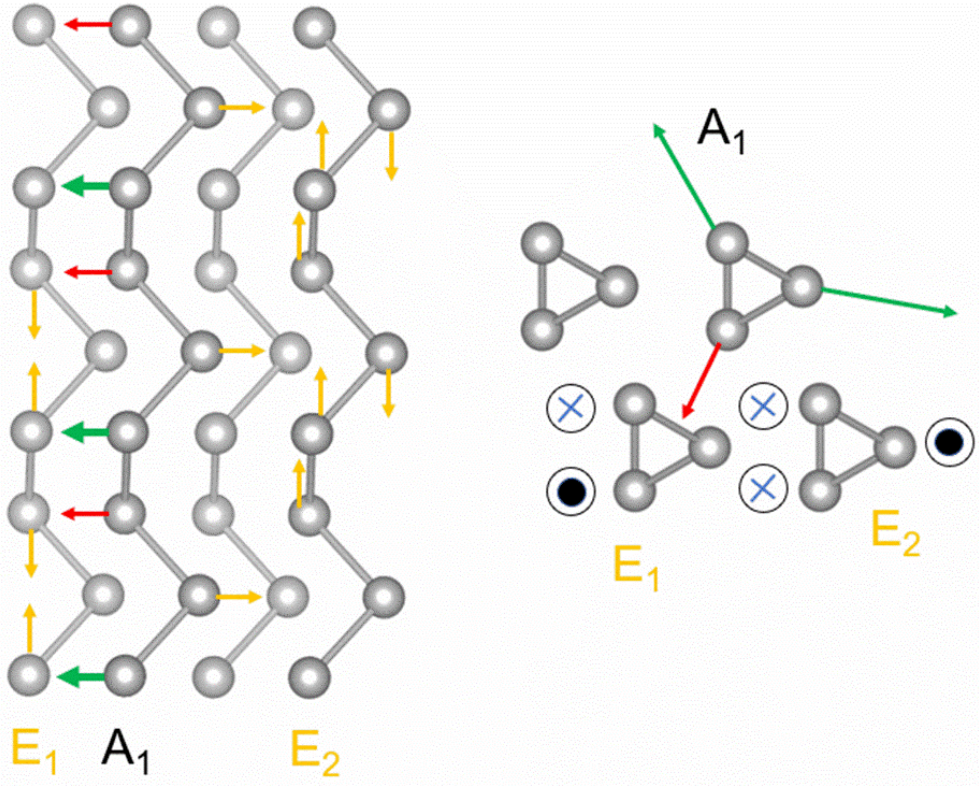

Fig. S2 Schematic shows the three Raman-active modes in helical-chain van der Waals material Te.

Supporting Note 3. Polarized Raman analysis

Theoretically, Te crystallizes with space group D_3^4 (or D_3^6) having three atoms per unit cell arranged helically along *c*-axis.[Rs1] The polarization Raman intensity of E_1-TO, A_1 and E_2 Raman modes can be expressed as.[Rs2]:

$$I_{E_1-TO,\perp} = |A\sin^2(\theta)|^2 + B \quad (1)$$

$$I_{A_1,\parallel} = |C\sin^2\theta + D\cos^2\theta|^2 + E \quad (2)$$

$$I_{E_2,\parallel} = |2F\sin(\theta + G)\cos(\theta + G)|^2 + H \quad (3)$$

where *A, B, C, D, E, F, G, H* are the Raman tensor elements and θ is the angle between the long-axis of Te nanoflakes and the incident light polarization direction.

Supporting Note 4. Te nanoflakes field effect transistor characteristic

Electrical performance of Te-based field-effect transistor (FET) was measured by a Keithley 4200A semiconductor characterization system. Back-gated FETs were fabricated on a heavily doped Si substrate with a 300 nm SiO_2 layer. and (see Materials and Method for details). The output characteristics (I_{ds}-V_{ds}) are shown in Fig. S3a nonlinear increased as the gate voltage decreasing from 0 to -50 V, indicating an ohmic contact between Cr/Au (10/100 nm) and Te channel. In addition, the transfer curve (I_{ds}–V_{gs}) shows the *p*-type behavior of Te channel in Figure S3b. The mobility of Te nanosheet is further estimated from the transfer curve measured at V_{ds} = 1 V using equation expressed by:

$$\mu = \frac{L}{WC_iV_{ds}}\frac{\partial I_{ds}}{\partial V_g}$$

where L and W are the channel length and width, respectively, and C_i is the capacitance per unit area to the gate electrode ($C_i = \varepsilon_{SiO2}/d_{SiO2}$ = 1.23 × 10^{-4} F m^{-2} with ε_{SiO2} and d_{SiO2} is the dielectric constant and thickness of the SiO_2 substrate). As shown in Fig. S3(b), the hole mobility at room temperature is calculated to be 48.63 $cm^2/(Vs)$. The smaller mobility may be influenced by the presence of carriers near the semiconductor-oxide interface.

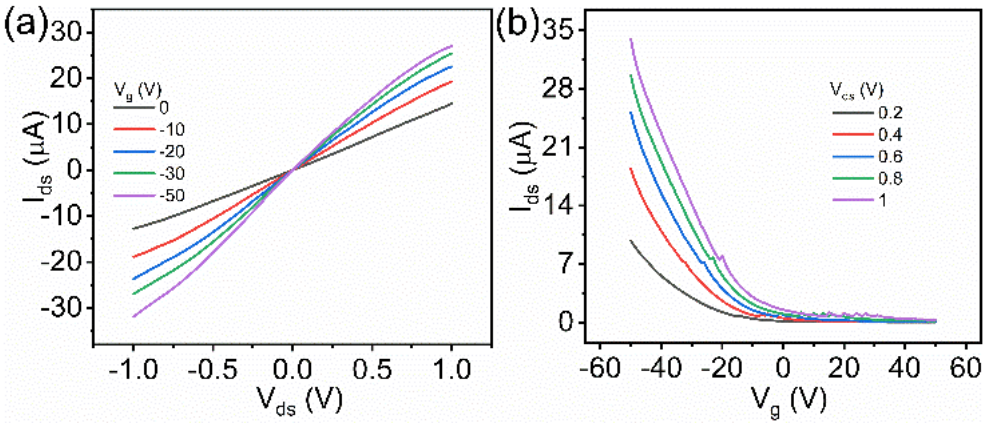

Fig. S3 (a) Output curves of Te flakes measured at different gate voltages. (b) Transfer curves of Te flakes measured under different source-drain voltages.

Supporting Note 5. Te nanoflakes short-wave infrared photodetector performance

Figure S4a shows the *I-V* curves of Te-based device under dark and different incident laser power density. Figure S4b and S4c shows the corresponding photo-switching behavior, which exhibits fast response (τ_{rise} ~33 μs and τ_{decay} ~30 μs) under different laser frequencies. As shown in Figure S4d, the stability of Te-based phototransistor is examined by switching the laser on and off for over 10 minutes, during which the photo-switching behavior exhibits no obvious degradation.

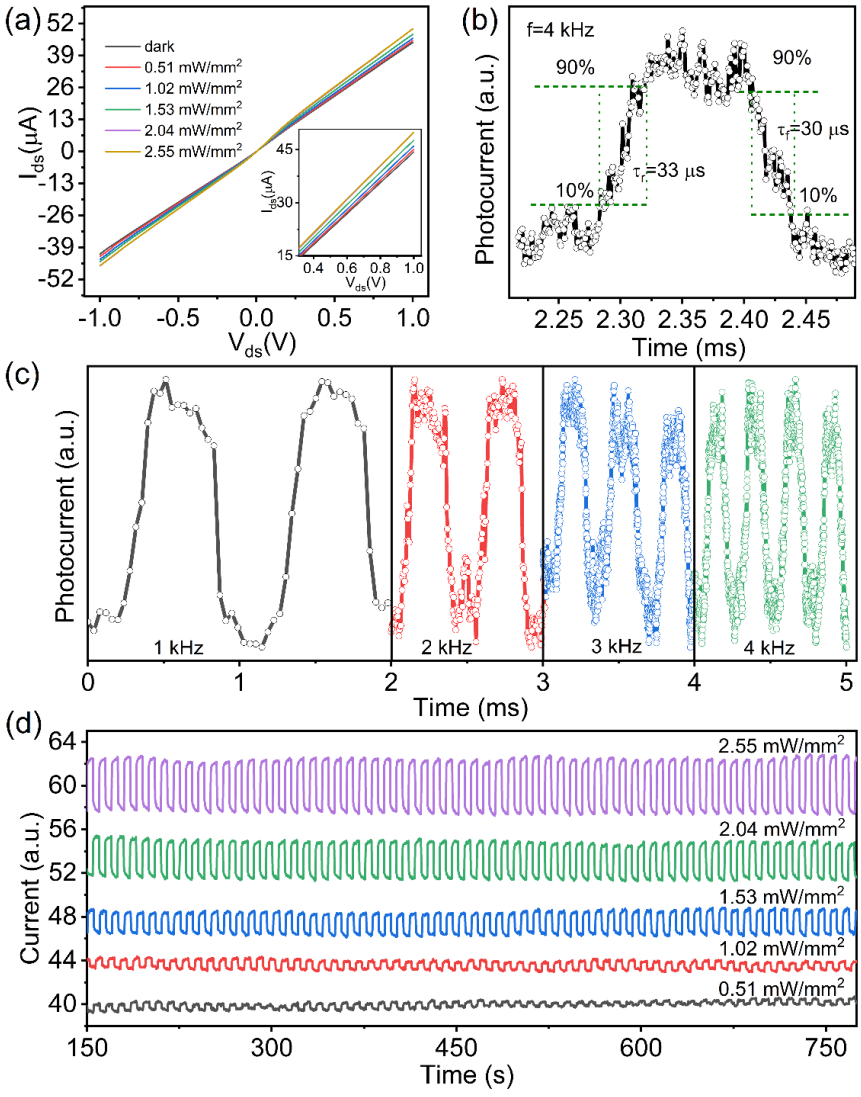

Fig. S4 (a) *I-V* curves of Te-based phototransistors under different laser power densities. (b) *I-t* curves as light turned on and off at different frequencies, with bias voltage of 1 V and incident light power of 2.04 mW/mm^2. (c) Response time of Te-based phototransistors. (d) Photo-switching behavior of Te-based phototransistors under different laser power densities. Excitation laser wavelength of 1550 nm.

Table S1 Performance Parameters Comparison of Photodetectors based on Te and other two-dimensional materials Photodetectors Reported in the Literature.

Materials	Detectivity (Jones)	Responsivity ($A\ W^{-1}$)	Rising time (ms)	Decay time (ms)	Refs
Te nanosheet	1.886×10^{10}	51.9	0.019	0.021	This work
Te flake	2×10^{9}	16	--	--	Rs3
Te nanosheet	10^{7}	1.34×10^{-5}	570	6400	Rs4
Te hexagonal flake	--	389.5	4400	2800	Rs5
Te nanosheet	--	9.38	0.07	0.072	Rs6
Te nanowire	1.23×10^{12}	6500	0.0317	0.0255	Rs7
PtSSe	--	--	0.0699	0.0319	Rs8
MoS_2	--	880	600	9000	Rs9
WS_2	--	$2.1X10^{-5}$	5.3	5.3	Rs10
GaS	10^{10}	4.2	30	--	Rs11
InSe	10^{11}	1.2	50	4000	Rs12
SnS_2	--	--	42	42	Rs13
$Ga_2In_4S_9$	$2.25x10^{11}$	111.9	40	50	Rs14
PtSe/GaAs	$2.52x10^{12}$	0.262	0.006	0.007	Rs15
Graphene/Si	$1.4X10^{8}$	$0.435x10^{-3}$	1.3	3	Rs16
PdSe/Si	$1.18x10^{13}$	0.3	0.038	0.044	Rs17

REFERENCES

(Rs1) A. S. Pine, G. Dresselhaus, *Phys. Rev. B.* 1971, **4,** 356-371.

(Rs2) L. Tong, X. Huang, P. Wang, L. Ye, M. Peng, L. An, Q. Sun, Y. Zhang, G. Yang, Z. Li, F. Zhong, F. Wang, Y. Wang, M. Motlag, W. Wu, G. J. Cheng and W. Hu, *Nat. Commun.,* 2020, **11,** 2308.

(Rs3) M. Amani, C. Tan, G. Zhang, C. Zhao, J. Bullock, X. Song, H. Kim, V.R. Shrestha, Y. Gao, K.B. Crozier, M. Scott and A. Javey, *ACS Nano.,* 2018, **12,** 7253-7263.

(Rs4) J. Peng, Y. Pan, Z. Yu, Jia. jing. Wu, Jun. chi. Wu, Yuan. Zhou, Yu. qiao. Guo, Xiao. jun. Wu, Chang. zheng. Wu, and Yi. Xie, *Angew. Chem. Int. Ed.,* 2018, **57,** 13533-13537.

(Rs5) Q. Wang, M. Safdar, K. Xu, M. Mirza, Z. Wang and J. He, *ACS Nano.,* 2014, **8,** 7497-7505.

(Rs6) W. Ma, Y. Gao, L. Shang, W. Zhou, N. Yao, L. Jiang, Q. Qiu, J. Li, Y. Shi, Z. Hu and Z. Huang, *Adv. Sci.,* 2022, **9,** 2103873.

(Rs7) M. Peng, R. Z. Xie, Z. Wang, P. Wang, F. Wang, H. N. Ge, Y. Wang, F. Zhong, P. S. Wu, J. F. Ye, Q. Li, L. L. Zhang, X. Ge, Y. Ye, Y. C. Lei, W. Jiang, Z. G. Hu, F. Wu, X. H. Zhou, J. S. Miao, J. L. Wang, H. G. Yan, C. X. Shan, J. N. Dai, C. Q. Chen, X. S. Chen, W. Lu, W. D. Hul, *Sci. Adv.,* 2021, **7,** eabf7358.

(Rs8) Z. Wang, H. Xia, P. Wang, X. H. Zhou, C. S. Liu, Q. H. Zhang, F. Wang, M. L. Huang, S. Y. Chen, P. S. Wu, Y. F. Chen, J. F. Ye, S. Y. Huang, H. G. Yan, L. Gu, J. S. Miao, T. X. Li, X. S. Chen, W. Lu, P. Zhou, and W. D. Hu, *Adv. Mater.,* 2021, **33,** 2104942.

(Rs9) O. Lopez-Sanchez, D. Lembke, M. Kayci, A. Radenovic, A. Kis, *Nat. Nanotechnol.,* 2013, **8,** 497.

(Rs10) N. Perea-López, A. L. Elías, A. Berkdemir, A. Castro-Beltran, H. R. Gutiérrez, S. Feng, R. Lv, T. Hayashi, F. López-Urías, S. Ghosh, B. Muchharla, S. Talapatra, H. Terrones, M. Terrones, *Adv. Funct. Mater.*, 2013, **23,** 5511.

(Rs11) P. Hu, L. Wang, M. Yoon, J. Zhang, W. Feng, X. Wang, Z. Wen, J. C. Idrobo, Y. Miyamoto, D. B. Geohegan, K. Xiao, *Nano Lett.*, 2013, **13,** 1649.

(Rs12) S. R. Tamalampudi, Y. Y. Lu, U. R. Kumar, R. Sankar, C. D. Liao, B. K. Moorthy,

C. H. Cheng, F. C. Chou, Y. T. Chen, *Nano Lett.,* 2014, **14**, 2800.

(Rs13) J. Xia, D. Zhu, L. Wang, B. Huang, X. Huang, X. M. Meng, *Adv. Funct. Mater.*, 2015, **25,** 4255.

(Rs14) F. k. Wang, T. Gao, Q. Zhang, Z. Y. Hu, B. Jin, L. Li, X. Zhou, H. Q. Li, Gustaaf. Van. Tendeloo, and T. Y. Zhai. *Adv. Mater.,* **2018,** 1806306.

(Rs15) X. An, F. Liu, Y. J. Jung and S. Kar, *Nano Lett.,* 2013, **13,** 909-916.

(Rs16) C. Jia, D. Wu, E. Wu, J. Guo, Z. Zhao, Z. Shi, T. Xu, X. Huang, Y. Tian and X. Li, *J. Mater. Chem. C.,* 2019, **7,** 3817-3821.

(Rs17) L. Zeng, D. Wu, S. Lin, C. Xie, H. Yuan, W. Lu, S. P. Lau, Y. Chai, L. Luo, Z. Li and Y. H. Tsang, *Adv. Funct. Mater.,*2019, **29,** 1806878.